BDNF-induced axonal mTOR activation promotes Rab5 translation, axonal transport, and CREB phosphorylation in cortical neurons.

Tiburcio-Felix Reynaldo[1], Tapia-Peralta Constanza[1], Arriagada Gloria[1], Perlson Eran[2], Bronfman Francisca C[1].

[1]Institute of Biomedical Sciences (ICB), Faculty of Medicine, and Faculty of Life Sciences, Universidad Andrés Bello, Santiago, Chile.

[2]Department of Physiology and Pharmacology, Sackler Faculty of Medicine, Sagol School of Neuroscience, Tel Aviv University, Tel Aviv, Israel.

Acknowledgement: The authors gratefully acknowledge financial support from ANID (Agencia Nacional de Investigacion y Desarrollo), FONDECYT grant no. 1221203 to FCB, FONDECYT grant no. 1220480 to GA. DI-04-24/NUC from Universidad Andres Bello to G.A. and FCB. FONDECYT postdoctoral grant no. 3200800 and a postdoctoral grant from Secretaria de Educación, Ciencia, Tecnología e Innovación de la Ciudad de México (SECTEI) sectei/113/2022 to RTF.

ABSTRACT

Neuronal plasticity, essential for learning and memory, involves structural changes triggered by neurotrophic factors such as brain-derived neurotrophic factor (BDNF). BDNF activates its receptor, TrkB, to induce local and long-distance signaling, promoting dendritic branching. While BDNF activation of the mechanistic target of rapamycin (mTOR) pathway is well-documented in dendritic spines, its role in axons remains unclear. Using compartmentalized cultures of embryonic cortical neurons from mice, this study demonstrates that axonal BDNF triggers mTOR-dependent phosphorylation of translation regulators (4E-BP1 and S6), driving local protein synthesis. Fluorescent labeling, immunostaining, and radial microfluidic chambers were employed to isolate axonal compartments and assess local translation. Axonal BDNF increased Rab5 protein translation in a TrkB- and mTOR-dependent manner, highlighting the importance of localized protein synthesis for axonal trafficking.

Furthermore, axonal protein synthesis was required for retrograde transport of internalized cargoes and CREB activation in the nucleus, linking local translation to long-distance signaling. These findings highlight the crucial role of axonal mTOR activation in regulating local proteostasis and neuronal function, offering new insights into axonal trafficking mechanisms and their implications for neuroplasticity. This work advances our understanding of how mTOR activation in axons and localized translation induced by BDNF are essential for axonal transport and efficient signaling in cortical neurons.

INTRODUCTION

Neuronal plasticity, the ability of neurons to adapt and reorganize, is fundamental to processes such as learning and memory. This plasticity is driven by rapid structural changes in synapses, including dendritic and axonal growth, which are regulated by neuronal activity and neurotrophic factors (NTFs). Among NTFs, brain-derived neurotrophic factor (BDNF) is the most extensively studied in the central nervous system (CNS). BDNF is secreted in an activity-dependent manner by neurons to activate its receptor, the tropomyosin receptor kinase B (TrkB). Upon activation, TrkB induces local cytoskeletal changes and long-distance signaling that influence nuclear gene expression, thereby supporting synaptic remodeling and circuit maintenance (*1, 2*).

Recent studies, including our own, have shown that BDNF signaling in cortical neuron axons forms specialized signaling endosomes that contain BDNF and activated TrkB (*3-7*). These endosomes facilitate axon-to-nucleus communication, promoting cAMP response element binding protein (CREB)-dependent transcription of plasticity-related genes, such as *Arc*, and enhancing dendritic branching. This mechanism highlights the critical role of signaling endosomes in maintaining neuronal circuits.

Rab GTPases, key regulators of membrane trafficking, play a pivotal role in orchestrating the dynamics of BDNF/TrkB signaling endosomes. Rab proteins act as molecular switches, cycling between GDP- and GTP-bound states, and recruit effectors to specific membrane compartments. Rab5 mediates the first step of receptor sorting and vesicle fusion in early endosomes, Rab11 facilitates receptor recycling, and Rab7 governs the transition to late endosomes (*8-10*). These Rab-mediated processes are essential for neurotrophin signaling, connecting signal transduction with endosomal trafficking. Our previous findings reveal that BDNF enhances the activity of Rab5 and Rab11 in hippocampal neurons, and that reduced Rab function impairs BDNF-induced dendritic arborization (*11-13*).

Rab5 and Rab7 activity regulate long-distance neurotrophin signaling in axons, underscoring the critical role of Rab5 in axonal transport. In motoneurons, Rab5 facilitates early sorting of TrkB, while Rab7 predominates in axonally transported vesicles (*14*). Similarly, Rab7-positive endosomes transport NGF/TrkA complexes in sympathetic neurons, influencing survival. Rab5 activity is also linked to axonal BDNF signaling endosomes that mediate cell death in sympathetic neurons (*15-17*). In cortical neurons, Rab5 retrograde transport is regulated by the dynein effector Hook, and TrkB is transported in Rab7-positive endosomes in hippocampal neurons (*18-20*). Altogether, these data indicate that trafficking through Rab5-early endosomes is a critical step in regulating receptor axonal transport in CNS axons.

BDNF binding to TrkB induces receptor dimerization and phosphorylation of tyrosine residues, creating docking sites for adaptor proteins. This phosphorylation activates signaling cascades such as ERK1/2, PI3K-AKT, and PLCγ-Ca^{+2}, leading to CREB activation and dendritic arborization (*1, 21*). Additionally, BDNF facilitates protein

translation via the mechanistic target of rapamycin (mTOR) pathway, which is crucial for dendritic growth and synaptic plasticity. mTOR, a conserved serine/threonine kinase, regulates protein synthesis, cell growth, autophagy, and neuronal excitability. In neurons, mTOR forms two distinct complexes: mTORC1, which drives mRNA translation, and mTORC2, which regulates cytoskeletal reorganization and cell survival (*22-24*).

Activation of mTORC1 leads to phosphorylation of substrates such as eIF4E binding proteins (4E-BP1) and the ribosomal S6 kinases (S6Ks), key proteins that control translation initiation (*25*). Local protein synthesis in axons and dendrites supports neuronal development and function, enabling rapid responses to stimuli. Indeed, disruptions in local proteostasis are linked to neurodegenerative and neurodevelopmental diseases (*26-29*). While BDNF activation of mTOR is well-documented in dendritic spines, its role in axons remains poorly understood (*22, 23*).

Using compartmentalized cultures of mouse cortical neurons, we demonstrate that axonal BDNF triggers mTOR-dependent phosphorylation of 4E-BP1 and S6, driving local protein synthesis. This process enhances axonal transport and CREB phosphorylation in the nucleus. Specifically, BDNF increases Rab5 protein translation in a TrkB- and mTOR-dependent manner. These findings underscore the importance of localized protein synthesis in regulating neuronal development and function, providing new insights into axonal trafficking and signaling mechanisms.

RESULTS

BDNF in axons of cortical neurons increases local protein synthesis in a mTOR-dependent manner.

Different lines of evidence have indicated that BDNF can activate mTOR in dendrites and spines (*22, 23*). So far, no studies have addressed the functional role of axonal local protein translation mediated by BDNF-TrkB-mTOR in CNS neurons. To investigate whether BDNF increases mTOR activity in axons, we employed an *in vitro* model of compartmentalized cultures of cortical neurons, which has been validated in various studies (*7, 30-32*). In brief, we prepared cortical neurons plated in microfluidic devices with 300 µm long microgrooves. In these cultures, axons can reach up to 1400 µm, which is 70-90 times longer than the diameter of neuronal cell bodies, and can be divided into three regions based on their proximity to cell bodies. These regions are the axons in the microgrooves (MG), proximal axons (PA), and distal axons (DA) (Figure 1A and B). After six days in vitro (DIV6), we added a fluorescent version of subunit B of cholera toxin (f-Ctb), which is internalized in axons and retrogradely transported up to the cell body of neurons with axons in the axonal compartment (AC). These step is required to label neurons with axons in the axonal compartments and to verify proper compartmentalization of the cultures. Then, at DIV7, before adding BDNF treatment, the TrkB-fc chimeric protein is added for 1 hour in the cell body compartment (CB) to neutralize the activity of endogenous BDNF released by neurons (*33*). Then, we treat the AC with BDNF for 3 hours. After, the neurons are fixed and immunostained against ßIII-tubulin to label axons (Figure 1A and B). In these conditions, when BDNF was added to axons, increased labeling for the mTOR targets phosphorylated S6 ribosomal protein (pS6) and eukaryotic translation initiation factor 4E-binding protein 1 (p4EBP1) by about 30% and a two-fold increase, respectively, was observed along the axons (Figure 1C-F and Supplementary Figure 1A-F). Increased pS6 and pEBP1 by BDNF were downregulated by Torin 1, a specific inhibitor of mTOR (*34*), and quantified from PA (Supplementary Figure 1G-I) and DA (Figure 1C-F). This suggests that the increased phosphorylation of mTOR targets induced by BDNF is mTOR-specific and also indicates the specificity of the immunostaining. To further explore whether increased phosphorylation of mTOR targets by BDNF resulted in increased general protein translation, we treated the axons with BDNF in the presence of O-propargyl-puromycin (OPP) (Figure 2A). After fixation, we performed a Click-it chemistry assay to label newly synthesized proteins fluorescently. This assay has been documented to label new proteins since puromycin is incorporated into nascent peptides (*35*). As expected, axonal BDNF increased the local translation of proteins in axons, observed as a 2-fold increase in fluorescence, which was reduced by Torin 1 and the translation inhibitor cycloheximide (CHX) (Figure 2), indicating that BDNF in axons triggers the synthesis of newly synthesized proteins in an mTOR-dependent manner.

Local protein synthesis induced by BDNF in cortical neurons is required for axonal transport and CREB phosphorylation.

Recently, we have reported that BDNF can increase the axonal retrograde transport of f-Ctb in cortical neurons (*30*). Indeed, the co-incubation of f-Ctb and BDNF for 3 hours resulted in twice the amount of f-Ctb transported to somas (Figure 3A-C). The BDNF-induced retrograde transport of f-Ctb was reduced to basal levels when axons were treated

with BDNF in the presence of anysomicine, a drug that reduces the translation of proteins (*36*) (Figure 3B and C). This result suggests that the retrograde transport of f-Ctb induced by axonal BDNF depends on the newly synthesized proteins in axons.

Different lines of evidence, from our studies and others, have indicated that f-Ctb is co-transported in axons with BDNF/TrkB signaling endosomes (*7, 37, 38*). Additionally, we have previously demonstrated that the retrograde transport of BDNF/TrkB signaling endosomes from axons to cell bodies enhances the phosphorylation of CREB. These processes resulted in the expression of plasticity genes such as *Arc* and dendritic arborizations (*7*). To address whether increased phosphorylation of CREB by axonal BDNF in compartmentalized cultures of cortical neurons requires new protein synthesis in axons, we compared the levels of nuclear pCREB in cultures treated with BDNF or BDNF in the presence of CHX (Figure 4A). Consistent with the requirement of local protein translation in axons for the propagation of signaling endosomes, the levels of pCREB were reduced in cultures treated with BDNF and CHX in axons (Figure 4B and C).

Axonal BDNF increases the local translation of Rab5 in a TrkB and mTOR-dependent manner.

Various lines of evidence suggest that small monomeric GTPases, such as RhoA, cdc42, and TC10, are locally translated in peripheral growth cones and axons in response to specific stimuli (*39-41*). Previous work from our lab demonstrated that BDNF enhances both the activity and the protein levels of Rab5 in an mTOR-dependent manner in hippocampal neurons (*11*). Based on these findings, we hypothesized that Rab5 is locally translated in axons of cortical neurons. First, we evaluated the levels of Rab5 in the absence or presence of BDNF in axons using immunofluorescence, as shown in Figures 5A-C. BDNF almost triple the levels of Rab5 in distal axons. This increment was reduced to basal levels by the addition of CHX to distal axons (Figure 5B and C). To obtain further evidence that Rab5 is synthesized in axons in response to BDNF, we studied the effect of BDNF on axons using radial chambers (Figure 6D), as has been performed before (*42*). These cultures allow the preparation of axonal protein homogenates separated from cell bodies (Figure 6D). We were able to detect the Rab5 protein in axonal lysates (Figure 6D). As expected from the immunofluorescent result of the figures mentioned above, the levels of axonal Rab5 were upregulated by BDNF and decreased by CHX (Figure 6E and F). To investigate further the specificity of the BDNF effect on increasing the protein levels of Rab5 we analyzed this effect on primary cultures of neurons derived from the $TrkB^{F616A}$ mice. This knock-in transgenic line expresses a mutation in the tyrosine kinase domain of TrkB that renders the receptor susceptible to inhibition by the drug 1NM-PP1 (*43*). The increment of Rab5 in distal axons was reduced by 1NM-PP1 and also by Torin1 (Figure 6A-C), indicating that the effects were dependent on both the activity of TrkB and mTOR. These results suggest that the BDNF-dependent increase of Rab5 levels in distal axons requires newly synthesized proteins and depends on the activity of TrkB and mTOR.

These results indicate that Rab5 is locally synthesized in axons and, therefore, the mRNA of Rab5 should be present in axons. To address this possibility, we prepared cDNA from axonal or cell body mRNA using radial chambers. Using RT-qPCR, we could find Rab5 mRNA in axons (AC) and in cell bodies (CB) as expected (Figure 7A and B). A proper control was used to show that there is no contamination in axonal lysates with mRNAs that should specifically distribute to cell bodies, such as polymerase B mRNA, which is a nuclear protein (Figure 7A and B). To get further evidence that BDNF increases the protein levels of Rab5 in axons by increasing newly translated Rab5 and considering that Rab5 mRNA is present in axons, we treated the axons with puromycin in the presence or absence of BDNF. Then, we performed a proximity ligation assay using antibodies against puromycin and Rab5 (Puro-PLA for Rab5) (*35*). Puro-PLA for Rab5 was increased in the presence of BDNF and reduced when treating axons with CHX (Figure 7C and D), indicating that BDNF increases the local translation of Rab5 in axons.

Altogether, our results indicate that BDNF in axons increases mTOR-dependent local translation of protein, particularly of Rab5, and that local translation is required for the effects of BDNF on increasing axonal transport and CREB phosphorylation in the nucleus. Given the pivotal role of Rab5 in sorting endosomes into the retrograde transport pathway (*14, 19, 44*), it is plausible that BDNF-induced Rab5 upregulation facilitates the axonal transport of internalized cargoes, thereby supporting efficient neuronal communication and cargo trafficking.

DISCUSSION

The role of the BDNF/mTOR signaling pathway in local translation in dendritic spines regulating synaptic plasticity is well proven (*45*); however, the role of this process in BDNF-mediated long-distance signaling in axons has not been established. Here, we show that BDNF in axons increases the activation of axonal mTOR signaling pathway and local translation of proteins, and that this process is required for BDNF-increased retrograde transport of f-Ctb and CREB phosphorylation in the soma of compartmentalized cortical neurons. Furthermore, we provide compelling evidence that one of the proteins locally translated in axons by BDNF is Rab5, a key monomeric GTPase regulating endosomal transport.

Our lab, along with others, has investigated the role of various signaling pathways triggered by BDNF/TrkB in axons. Notably, PLCγ-Ca^{+2} signaling is essential for the internalization of the BDNF/TrkB complex into axonal endosomes (*30*). On the other hand, ERK1/2 signaling has been shown to modulate and phosphorylate dynein subunits, thereby enhancing the retrograde transport of the BDNF/TrkB complex (*46*). In contrast, activation of PI3K in axons does not influence the internalization or transport of BDNF/TrkB but is critical for cellular responses to signaling endosomes, such as dendritic arborization (*7*). Here, we demonstrate that axonal BDNF stimulates mTOR-dependent protein synthesis, which is necessary for both the increased retrograde transport of f-Ctb and the phosphorylation of the transcription factor CREB. Previously, we showed that the retrograde activation of CREB by axonal BDNF is essential for promoting dendritic arborization processes that rely on the retrograde transport of signaling endosomes (*7*). Furthermore, we found that axonal BDNF not only boosts the transport of signaling endosomes but also enhances the transport of f-Ctb (*30*), suggesting that BDNF activates broader endosomal pathways. These findings align with earlier studies indicating that elevated axonal calcium levels enhance the retrograde transport of both TrkB and f-Ctb in cortical neurons (*37*). To our knowledge, this is the first report indicating that mTOR-mediated local translation is required for retrograde BDNF signaling and thus advances our understanding of the cellular mechanism driving long-distance communication in neurons of the CNS. Indeed, as discussed below, most examples of local translation in the CNS report local function at the growth cones during development or at the presynaptic terminals in the developing CNS.

Neurons regulate their proteome to support the specialized functions of subcompartments such as synapses, dendrites, and axons. By transporting mRNAs to axons, neurons enable localized protein synthesis, providing spatial and temporal control over protein production and activity. The presence of axonal mRNA and local translation in axons of the peripheral nervous system is well established, and it plays a key role in injury responses and the regeneration of peripheral neurons, such as sensory neurons (*28, 47*). On the other hand, the role of local translation in axons of the CNS is less described. One of the most studied

mRNAs in CNS neurons is β-actin mRNA, which was uncovered and localized to growth cones in chick forebrain neurons (*48*). Indeed, local translation of β-actin is required for axonal arborization of developing retinal ganglion cells (RGC) (*49*). Axonal mRNAs have also been characterized in compartmentalized cultures of cortical neurons, including changes following axotomy (*50*). In hippocampal cultures, the axonal endoplasmic reticulum facilitates local translation, a process regulated by neurotrophins (*51*). *In vivo*, active translation in axons of the visual circuit during development and adulthood has been demonstrated (*52*). In addition, BDNF is known to positively regulate the local protein synthesis in the growth cone of developing axons, inducing specific proteomes (*49, 53*). Also, local protein synthesis in presynaptic compartments is now considered a widespread feature of the adult brain, with over 400 transcripts identified in glutamatergic terminals via RNA-seq and subcellular fractionation (*54*). Local translation of SNAP25 is required for the formation of presynaptic terminals (*55*), and in pyramidal cortical neurons, mTOR-mediated local translation regulates presynaptic NMDA receptor-dependent sustained firing (*56*). Moreover, transcriptomic and proteomic profiling of growth cones from callosal-projecting axons revealed enrichment of mTOR kinase and mRNAs containing mTOR-dependent motifs (*57*). The role of axonal mTOR-mediated translatome on neuronal function and mTOR activity as a requirement for the intrinsic ability of axons to regenerate has long been suggested to play a key role in axonal maintenance and axonal regeneration (*58-60*). Thus, our new findings highlight a new role of axonal mTOR in long-distance signaling mediated by BDNF.

Rab5, localized to early endosomes, is a key regulator of endocytic trafficking, controlling cargo selection, endosome fusion, motility, and signaling (*61, 62*). It is considered the master regulator of endocytic trafficking of receptors and their cargoes (*63, 64*). In both mice and humans, Rab5 exists as three homologs—Rab5A, Rab5B, and Rab5C—encoded by separate genes (*65*). Triple knockout of Rab5 isoforms leads to cell death and the loss of both early and late endosomes in vitro and *in vivo* (*66-68*). Interestingly, malfunction of the early endocytic pathways is associated with several neurodegenerative diseases, including Alzheimer´s and amyotrophic lateral sclerosis (ALS) (*69-71*). Particularly in axons, Rab5-Rab7 transitions regulate BDNF/TrkB transport since in motor neurons Rab5 facilitates early sorting of TrkB (*14*). In cortical neurons, the dynein effectors regulate Rab5 retrograde transport, and TrkB is transported in Rab7-positive endosomes in hippocampal neurons (*18-20*).

In this research, we demonstrate that Rab5 is locally translated in axons in an mTOR- and TrkB-dependent manner in response to BDNF. To our knowledge, this is the first report of regulated local translation of a Rab family member. Furthermore, the fact that Rab5 is essential for the retrograde transport and sorting of receptors, coupled with the requirement of local translation for BDNF-induced increases in retrograde transport and nuclear signaling, suggests that the local translation of Rab5 by BDNF likely enhances BDNF

retrograde transport, nuclear signaling, and dendritic arborization (*7*). Taken together, these findings indicate that mTOR-mediated local translation promotes Rab5 synthesis, thereby upregulating retrograde transport and amplifying long-distance signaling.

METHODS

Materials.

List of Materials in Supplementary Material.

Isolation and Culture of Embryonic Cortical Neurons.

Embryonic cortical neurons were isolated from C57Bl/6 J or TrkB^{F616A} knock-in mice (*43*) on embryonic days 16–17 and obtained from the animal facilities of our institution. Pregnant animals were euthanized under deep anesthesia following bioethical protocols approved by the Bioethics Committee of the Universidad Andrés Bello (009/2022).

Preparation and Cell Culture.

Cortical tissues from mice were dissected and dissociated into single cells in Hank's balanced salt solution (HBSS). After dissociation, the neurons were resuspended in Modified Dulbecco's Modified Eagle Medium (DMEM) supplemented with 10% horse serum (HS) (DMEM/HS) and seeded in microfluidic chambers at a density of 50,000 cells/microfluidic chamber. Three hours later, the culture medium was replaced with complete neurobasal supplemented with 2% B27, 1x GlutaMAX, and 1x penicillin/streptomycin, as well as 0.25 μM cytosine arabinoside (Ara-C).

Compartmentalized cultures.

The molds used to prepare standard two-chamber microfluidic cultures, as previously published (*4, 38*), and radial compartmentalized chambers, as published in Altman et al. 2021(*42*) were fabricated at the microfluidic core facility of Tel Aviv University (*72*). Microfluidic chambers were prepared using a SyldgardTM 184 silicone elastomer base, following the manufacturer's instructions. Two days before primary culture, glass coverslips (25 mm for the standard microfluidic chamber or 12 mm for the radial microfluidic chamber) were incubated overnight with poly-D-lysine (0.1 mg/mL). The next day, the poly-D-lysine was washed with MilliQ-ultrapure water, and microfluidic chambers were placed on the dry coverslips. Then, laminin (2 μg/mL diluted in MilliQ-ultrapure water) was added to the chamber overnight. On the same day of the primary culture, the laminin solution was replaced with DMEM/HS (DMEM, supplemented with 10% Horse Serum, 1x GlutaMAX, and penicillin/streptomycin).

Standard two-chamber compartmentalized cultures were seeded at a density of 50,000 cells in the cell body compartment in 80 μL of DMEM/HS, and 160 μL of the medium was added to the axonal compartment. This procedure prevented cells from migrating to the axonal compartment. DMEM/HS is replaced three hours later by 160 μL of complete Neurobasal medium in the cell body compartment and 80 μL of complete Neurobasal medium in the axonal compartment. The differential volume between both compartments

must be at least 80–100 µL to ensure microfluidic isolation of the two compartments. This differential volume must be conserved throughout all cultures if fluidic isolation is required and to prevent evaporation. Every 48 hours, the culture medium is replaced with fresh, complete neurobasal medium, preserving the volume differential in both compartments. Experiments are performed on day in vitro (DIV) seven (DIV7).

For compartmentalized cultures in radial microfluidic chambers, 12-mm coverslips are placed in 24-well plates, treated with poly-D-lysine (0.1 mg/mL), and coated with laminin (2 µg/mL) as described for standard microfluidic chambers. Neurons were seeded at a density of 100,000 cells diluted in 60 µL of DMEM/HS and added to the central cell body compartment. On the other hand, 400 µL of DMEM/HS was added to the axonal (outside) compartment. After 3 hours, the DMEM/HS was replaced with complete neurobasal medium by adding 400 µL of medium to the axonal compartment and 100 µL to the cell body compartment. This volume differential allows for compartmentalization of the axonal compartment; volumes were adjusted every 48 hours. Compartmentalized cultures were used at DIV7 for RNA extraction to detect mRNA using RT-qPCR and for biochemical analyses of protein after BDNF treatment.

Axonal treatment with BDNF.

Each compartmentalized culture was evaluated for morphological and fluidic compartmentalization by using an axonal treatment with recombinant cholera toxin subunit B conjugated to Alexa Fluor 555 (f-Ctb) at a final concentration of 1 µg/mL. f-Ctb was added at DIV6 to the axonal compartment and allowed to incubate overnight. Experiments were conducted at DIV7. For standard microfluidic cultures, the cell media was removed from every compartment, and 160 µL of warm neurobasal media containing reduced levels of 0,5% of B27 (reduced neurobasal media) supplemented with TrkB-fc (100 ng/mL) was added to the cell body compartment. To the axonal compartment, 80 µL of warm reduced neurobasal media was added and allowed to incubate for 1 hour at 37ºC. Then, the media was replaced, specifically in the axonal compartment, with 80 µL of reduced neurobasal media supplemented with BDNF at 50 ng/mL, in the presence or absence of inhibitors, for 60-minute and 180-minute treatments. Afterward, the drugs were removed and washed twice with 120 µL of PBS supplemented with protease and phosphatase inhibitors.

Axonal immunostaining.

To fix neurons in standard compartmentalized cultures, the chamber was carefully removed, and 200 µL of a 4% paraformaldehyde and 4% sucrose solution diluted in PBS (PFA solution) was added to the coverslip for 18 min at room temperature (RT). Then, the PFA solution was removed, and three washes (5 minutes each) with 150 µL RT PBS were performed. Neurons were permeabilized with 150 µL of blocking solution (3% bovine serum albumin IgG and protease-free, BSA, 5%, fish gelatin, 0,2% saponin in PBS) for 60 min at RT. Appropriated primary antibodies were diluted in 100 µL of antibody solution

(BSA 3%, fish gelatin 5%, saponin 0,02% in PBS) and incubated overnight at 4 °C. The dilution for the first antibodies was as follows: rabbit anti-Rab5 (1:250), rabbit anti-phospho S6 (1:300), rabbit anti-phospho 4EBP1 (1:250), rabbit anti-phospho CREB (1:400), mouse anti-BIII-tubulin (1:750), and mouse anti-MAP2 (1:750). The next day, the primary antibody was removed, and three washes with 100 µL of PBS were performed, each for 5 minutes. The PBS buffer was removed, and neurons were incubated with 100 µL of secondary antibody dissolved in antibody solution for 90 min at RT. Donkey anti-rabbit Alexa 488 (1:500) and anti-mouse Alexa 647 (1:500) were used for experiments as secondary antibodies. The secondary antibody was removed, and coverslips were washed with cold PBS for 5 minutes. Then, samples were incubated with 100 µL of Hoechst solution (1:5000) for 10 min. The solution was removed, and cells were rewashed with cold PBS and then with cold distilled water to remove the salts. Finally, the coverslip was mounted in Mowiol.

Axonal phospho-S6 (pS6), phospho-4EBP1 (p4EBP1), and ß-III-tubulin protein quantification from cortical neurons by confocal microscopy.

Three independent experiments were conducted (corresponding to three different primary cultures), and three compartmentalized chambers were obtained from each experimental condition. Then, three fields per region in the axonal compartment (microgrooves, proximal, and distal regions) were captured with 63X magnification with a Leica SP8 confocal microscope in each compartmentalized chamber. To obtain the maximum fluorescence intensity projection, 5- to 8-stack images with a 1-µm separation between them were obtained. The fluorescence intensity per field was calculated by applying a threshold using the FIJI ImageJ version 1.5 software to eliminate the background from the microphotograph, which was then used to quantify the fluorescence associated with pS6 and p4EBP1, or OPP (see below). This value was standardized by ßIII tubulin levels, by dividing it by the fluorescent intensity obtained for the ßIII tubulin channel. The average of the three fields obtained for each region (microgrooves, proximal, and distal regions) was calculated to obtain the fluorescent intensity per region per chamber. The quantification was performed using the FIJI ImageJ version 1.5 software, and the protein of interest was plotted and standardized by ßIII tubulin levels.

Determination and quantification of BDNF-induced retrograde transport of f-Ctb. Neurons with axons in the axonal compartment (AC) were labeled by treating the AC with 1ug/ml f-Ctb in the presence or absence of BDNF (50 ng/ml) for 180 minutes. The effect of local translation for BDNF-induced retrograde transport of f-Ctb was assessed by treating the axons with anisomycin (25 uM). This treatment was initiated in the AC simultaneously with the depletion of endogenous BDNF with TrkB-Fc in the CB and kept for the next 180 minutes of BDNF treatment. Subsequently, the f-Ctb label is washed, and the cultures are fixed as indicated above. Mouse anti-MAP2 (1:750) was used as a cell marker. The cells were observed under epifluorescence microscopy.

The intensities of the f-Ctb fluorescence signals were initially quantified using ImageJ by subtracting the background autofluorescence of the label. This background was determined by measuring the intensity of images captured with a 555 filter under experimental conditions without the presence of Ctb. After background subtraction, regions of interest (ROIs) were generated for cells that displayed the Ctb label. Only cells containing more than three Ctb vesicles were included in the analysis. The selection tool was then used to demarcate areas with Ctb fluorescence, and fluorescence intensity values were measured for 45–50 cells per condition. The average Ctb intensity of the control condition was calculated, and each fluorescence intensity value from the experimental condition (+BDNF) was normalized by dividing it by the average intensity of the control condition.

Determination of phospho-CREB (pCREB) levels in the nucleus of compartmentalized cortical neurons.

Neurons with axons in the axonal compartment (AC) were labeled by treating axonal compartments ON with f-Ctb (Figure 1A and B). Then, the AC was treated with BDNF (50 ng/mL) in the presence or absence of cycloheximide (25 µM) for 180 min in the axonal compartment. After fixing the cultures, they were immunolabeled for pCREB (Ser 133). The fluorescence intensity of 15 cells per chamber labeled with f-Ctb was detected, from three independent experiments with two chambers each.

O-propargyl-puromycin (OPP) protein synthesis assay.

Standard compartmentalized cultures were used at DIV 7. The complete neurobasal medium was removed from the cell body compartment and was replaced with neurobasal supplemented with RS neurobasal medium containing TrkB-fc (100 ng/ml) for 60 min. In the last 30 minutes of this treatment, the complete neurobasal medium was replaced from the axonal compartment by RS neurobasal medium in the presence or absence of 25 µM cycloheximide (CHX) or 0.25 µM Torin1 for the remaining 30 min. Subsequently, the medium was removed from the axonal compartment and replaced with RS neurobasal medium supplemented with 20 µM OPP, with or without BDNF (50 ng/mL), and with or without CHX or Torin1 inhibitors for 60 min at 37°C. The medium was removed, and neurons were washed with RT PBS supplemented with protease inhibitors (100 uL/cover). Then, cells were fixed by adding RT PFA solution for 18 min. After removing PFA, the cells were washed twice with ice-cold PBS supplemented with protease inhibitors. Covers were incubated for 60 min in blocking solution, washed with ice-cold PBS, and then incubated with 50 µL of OPP detection mix based on click-iT chemistry according to the manufacturer's instructions. The cover was washed with 150 uL of cold PBS. The axonal tubulin was labeled with anti-ßIII tubulin (1:750) dissolved in antibody solution overnight at 4ºC and proceeded as described above for axonal immunostaining.

Determination of axonal mRNA.

Cortical neurons were cultured in radial microfluidic chambers. For this procedure, cells did not receive any treatment. RNA from axons and cell bodies was extracted from the outer and inner compartments of the radial microfluidic chambers, respectively, at DIV7, using the RNeasy kit following the instructions of the manufacturer. Ten chambers were required for each condition. Reverse transcription and qPCR were subsequently performed using the SuperScript™ First-Strand Synthesis System for RT-PCR with Oligo dT primers, according to the protocol of the manufacturer. Real-Time PCR was conducted to analyze the mRNA levels of polymerase B (PolB) (Fw: ACTTCACGTCAGAATCCAGC; Rv: CCTTTCCATCCTTCTCGCTG), Beta-actin (Fw: ACCTTCTACAATGAGCTGCG; Rv: CTGGATGGCTACGTACATGG), and Rab5 (Fw: CTATGCAGATGACAACAGCTT; Rv: TCAGTTACTACAACACTGGCT). Additionally, the ribosomal 18S gene (Fw: AGTCCCTGCCCTTTGTACACA; Rv: CGATCCGAGGGCCTCACTA) was used as a housekeeping gene.

Determination of Puro-PLA for Rab5.

Mouse cortical neuron compartmentalized cultures were treated with Ctb-F and TrkB as previously described. Puromycin (20 µM), with or without cycloheximide (25 µM), was added to axons for 60 minutes before BDNF treatment. Following this, axons were exposed to BDNF (50 ng/mL) or its absence for 180 minutes, with the previously added drugs maintained throughout the treatment. After the treatments, all reagents were removed, and the cultures were washed with cold PBS. The cells were then fixed and permeabilized as described in the Immunostaining section.

Proximity Ligation Assay (PLA) was performed using the NaveniFlex™ Cell MR kit the Navinchi, with rabbit anti-Rab5 and mouse anti-puromycin antibodies, incubated overnight at 4°C. Coverslips were subsequently mounted on slides with 20 µL of Mowiol. De novo synthesized Rab5 was visualized as dots after subtracting the background signal from a negative control lacking the primary antibodies. The number of dots was quantified using an SP8 confocal microscope at 63X magnification, acquiring maximum projections from 5–8 stacks with 1 µm separation.

Dot quantification per chamber was performed using FIJI ImageJ software with the "Analyze Particles" plugin, considering dots larger than 0.3 µm in diameter. The results were graphed as mean ± SEM, and statistical analysis was conducted using one-way ANOVA followed by a Bonferroni post-test.

Statistical Analysis

The results are expressed as the averages ± standard deviation (SD) or ± standard error of the mean (SEM), depending on the variability of the data. Student's *t*-test or one-way ANOVA followed by the appropriate multiple comparisons test was performed, depending on the number of groups used in each experiment. The details about the specific test used,

level of significance, and number of replicates are indicated in each figure legend. Statistical analyses were performed using GraphPad Prism 10 (Scientific Software).

FIGURE LEGENDS

Figure 1. BDNF induces mTOR-dependent phosphorylation of ribosomal protein S6 (pS6) and eukaryotic translation initiation factor 4E-binding protein 1 (4EBP1) in axons of compartmentalized cortical neurons. A. Experimental design and diagram of compartmentalized cultures of mouse cortical neurons in microfluidic chambers, used to study local BDNF-induced signaling. The cell body (CB) and axonal compartments (AC) are labeled. On DIV6, 1 µg/mL of fluorescent cholera toxin subunit B (f-Ctb) was added to the AC. The next day, TrkB-fc (100 µg/mL) was added only to the cell bodies for 60 minutes. Subsequently, BDNF (50 ng/mL) was applied to the axons for 180 minutes. **B.** Representative image of compartmentalized cultures on DIV7. ßIII-tubulin (red) and f-Ctb (green) were detected by confocal microscopy. The cell body compartment (CB), microgrooves (MG), proximal axons (PA), and distal axons (DA) are distinguished. Scale bar, 200 µm. **C and D.** Cortical neurons in compartmentalized cultures were treated with or without BDNF (50 ng/mL) and with or without the mTOR inhibitor Torin1 (0.25 µM). Fixed cultures were labeled for pS6 (green) in **C**, or p4EBP1 (green) in **D**, along with ßIII-tubulin (ßIII) in red. **E and F.** Quantification of immunofluorescence for pS6 in proximal axons (DA) in **E** and p4EBPA1 in **F**. Conditions include non-treated axons (control), axons treated with BDNF (BDNF), axons treated with Torin1 (Torin1), and axons treated with BDNF in the presence of Torin1 (BDNF + Torin1). Data represent the mean ± SD from n=9-10 chambers across three experiments. Statistical analysis was performed using one-way ANOVA and Bonferroni post-test (***p<0,001).

Figure 2. BDNF induces axonal protein synthesis in a mTOR and translation-dependent manner. A. The AC was treated with BDNF or vehicle (control) in the absence or presence of Torin1 (0,25 µM) and cycloheximide (CHX, 25 µM) for 180 minutes in the presence of O-propargyl-puromycin (OPP). OPP was visualized using click-it chemistry with a picolyl azide conjugate Alexa Fluor™ 488 dye and visualized using a magenta scale, as shown in the insets in A (last left panel). Axons were co-stained with an antibody against ß-III-tubulin (ßIII) (right panels), shown in red. **B.** Quantification of OPP fluorescence intensity (arbitrary units). Values represent mean ± SD of n=9-10 chambers from three independent experiments. Statistical analysis was performed using One-Way ANOVA and the Bonferroni post-hoc test (***p < 0.001).

Figure 3. Axonal BDNF increases the retrograde transport of f-Ctb, a process regulated by axonal local translation. A. Cortical neurons were cultured in microfluidic chambers up to day 7 (DIV7). Then, TrkB-fc (100 ng/mL) was added for 60 minutes of treatment in the CB compartment, the AC was treated or not with 25 µM anisomycin

(Aniso) for 1 hour before treating axons with or without BDNF (50 ng/mL) for 180 minutes in the presence of f-Ctb (1 µg/mL), as shown in red. Nuclei were stained with Hoechst (blue), and as a general neuronal marker, immunostaining against MAP2 was used, shown in green. **B.** The right panel shows the overlap of the f-Ctb and Hoechst channels, and the left panel shows the overlap of the three labels. **C.** Quantification of the f-Ctb-associated fluorescence intensity in cell bodies relative to the control. The white arrows indicate neuronal somas without the f-Ctb label, and the red arrows indicate somas of a neuron with the f-Ctb mark. Only cells with a f-Ctb were considered in the quantification. The values are expressed as the mean +/- SEM. n = 45-50 neurons from three independent experiments (3 different chambers per experiment). Statistical analysis was performed using one-way ANOVA and the Bonferroni post-hoc test (***$p < 0.0001$). Scale bar, 20 µm.

Figure 4. Inhibition of axonal translation decreases BDNF-induced retrograde signaling. A. Cortical neurons were cultured in microfluidic chambers as indicated in Figure and neurons having axons in the AC were labeled by adding f-Ctb (shown in red) to the AC ON. After 60 minutes of TrkB-fc (100 ng/mL) treatment in the CB compartment, the AC was treated or not with 25 µM cycloheximide (CHX) for 1 hour before treating axons with or without BDNF (50 ng/mL) for 180 minutes. Nuclei were stained with Hoechst (blue) and immunostained for pCREB (Ser133) shown in green, in cells labeled with f-Ctb. Scale bar 10 µm. **B.** Quantification of nuclear pCREB fluorescence intensity. Values represent mean ± SEM of 90 cells from three independent experiments. Statistical analysis was performed with One-Way ANOVA and Bonferroni post-test (***$p<0.001$).

Figure 5. The increment of Rab5 in distal axons induced by BDNF depends on protein translation. A. Cortical neurons were cultured in microfluidic chambers for 7 days. Then, TrkB-fc (100 ng/mL) was added for 60 minutes of treatment in the CB compartment. After, the AC was not treated (control) or treated with BDNF (BDNF), 25 µM of cycloheximide (CHX), or BDNF in the presence of CHX (BDNF + CHX). **B.** Rab5 immunostaining in control axons or axons stimulated with BDNF in the absence of CHX for 180 minutes. Pictures were obtained by confocal microscopy in distal axons. Scale bar 50µm**. C.** Quantification of Rab5 immunofluorescence intensity (green) in distal axons standardized by ßIII-tubulin (ßIII) immunostaining. Values represent the mean ± SD of n=9-10 chambers from three independent experiments. Statistical analysis was performed with one-way ANOVA and Bonferroni post-test. (***$p<0,001$). **D.** Left panel, scheme of a radial chamber used to obtain axonal (AC) and cell body (CB) lysates of cortical neurons. Right panel, lysates were characterized by the presence of a nuclear marker (Neu N), axonal marker (Tau), and the presence of Rab5. T, indicates total lysate, including cell bodies and axons. **E.** Cortical neurons were cultured in radial compartmentalized cultures up to day 7. Then, TrkB-fc (100 ng/mL) was added for 60 minutes in the CB compartment. After the AC was not treated or it was treated with BDNF, 25 µM of cycloheximide (CHX), or BDNF in the presence of CHX. Lysates were obtained from the AC (axonal

proteins), CB, and total proteins (T), and the levels of Rab5, Lamin A/C (nuclear marker), and βIII-tubulin (βIII) were assessed. CB or T lysates have no treatment. **F.** Quantification of axonal Rab5 normalized by ßIII. Values represent the mean ±SD, n=4. Statistical analysis was performed by one-way ANOVA and Bonferroni post-test (***p<0,001).

Figure 6. The increment of Rab5 in distal axons induced by BDNF depends on the activity of TrkB and mTOR. A. Cortical neurons were cultured in microfluidic chambers up to day 7. Then, TrkB-fc (100 ng/mL) was added for 60 minutes of treatment in the CB compartment. After, the AC was not treated or treated with BDNF (BDNF), 1NM-PP1 (1 µM), or BDNF in the presence of 1NM-PP1 (BDNF + 1NM-PP1) or Torin1 (BDNF + Torin1) for 180 minutes. **B.** Rab5 immunostaining in control axons or axons stimulated with BDNF in the absence or presence of TrkB and mTOR inhibitors (1NM-PP1 and Torin1). Neurons were labelled for axonal Rab5 GTPase, shown in green, and ßIII-tubulin (ßIII), shown in red. Pictures were obtained by confocal microscopy in distal axons. Scale bar 50µm. **C.** Quantification of Rab5 immunofluorescence intensity in distal axons standardized by ßIII-tubulin (ßIII) immunostaining. Values represent the mean ± SD of n=9-10 chambers from three independent experiments. Statistical analysis was performed with one-way ANOVA and Bonferroni post-test (****p<0,001).

Figure 7. Rab5 mRNA is localized to axons and is locally translated in response to BDNF. A. Cortical neurons were cultured in radial compartmentalized cultures up to day 7. Then, lysates obtained from the axonal compartment (AC) were analyzed by RT-qPCR using primers for Rab5 (targeting all Rab5 isoforms), ß-actin, polymerase B, and 18S RNA. The bands correspond to RT-qPCR products. **B.** RT-qPCR-based mRNA quantification of Rab5, ß-actin, and polymerase B relative to cell body levels of each gene. 18S RNA was used as a housekeeping gene. Values represent the mean ±SEM of four independent experiments. Statistical analysis was performed by T-Student (**p<0,05). **C**. Cortical neurons were grown in microfluidic chambers for six days. Then, TrkB-fc (100 ng/mL) was added for 60 minutes of treatment in the CB compartment. After, the AC was not treated (control) or treated with BDNF (BDNF), or BDNF in the presence of CHX (BDNF + CHX), in the presence of puromycin. Subsequently, the neurons were fixed, and immunostaining was performed for puromycin and Rab5, followed by PLA. De novo-synthesized Rab5 protein was observed in green, and the axons were labeled with f-Ctb in red. Scale bar, 10 µm. **D.** Quantification of PLA fluorescence (green) in distal axons for each treatment. n=9-10 compartmentalized chambers from three independent experiments. Statistical analysis was performed by one-way ANOVA and Bonferroni post-test. Results are expressed as mean ± SD. ***p<0,001.

BIBLIOGRAPHY

1. S. Finkbeiner *et al.*, CREB: a major mediator of neuronal neurotrophin responses. *Neuron* **19**, 1031-1047 (1997).
2. G. Leal, D. Comprido, C. B. Duarte, BDNF-induced local protein synthesis and synaptic plasticity. *Neuropharmacology* **76 Pt C**, 639-656 (2014).
3. C. Scaramuzzino, E. C. Cuoc, P. Pla, S. Humbert, F. Saudou, Calcineurin and huntingtin form a calcium-sensing machinery that directs neurotrophic signals to the nucleus. *Sci Adv* **8**, eabj8812 (2022).
4. G. Moya-Alvarado *et al.*, BDNF/TrkB signaling endosomes in axons coordinate CREB/mTOR activation and protein synthesis in the cell body to induce dendritic growth in cortical neurons. *Elife* **12**, (2023).
5. O. M. Lazo, G. Schiavo, Rab10 regulates the sorting of internalised TrkB for retrograde axonal transport. *Elife* **12**, (2023).
6. K. R. Sullivan, A. Ravens, A. C. Walker, J. D. Shepherd, "Arc - A viral vector of memory and synaptic plasticity". *Curr Opin Neurobiol* **91**, 102979 (2025).
7. G. Moya-Alvarado *et al.*, BDNF/TrkB signaling endosomes in axons coordinate CREB/mTOR activation and protein synthesis in the cell body to induce dendritic growth in cortical neurons. *eLife* **12**, e77455 (2023).
8. M. Zerial, H. McBride, Rab proteins as membrane organizers. *Nat Rev Mol Cell Biol* **2**, 107-117 (2001).
9. H. Stenmark, Rab GTPases as coordinators of vesicle traffic. *Nat Rev Mol Cell Biol* **10**, 513-525 (2009).
10. A. Wandinger-Ness, M. Zerial, Rab proteins and the compartmentalization of the endosomal system. *Cold Spring Harb Perspect Biol* **6**, a022616 (2014).
11. A. Gonzalez-Gutierrez, O. M. Lazo, F. C. Bronfman, The Rab5-Rab11 Endosomal Pathway is Required for BDNF-Induced CREB Transcriptional Regulation in Hippocampal Neurons. *J Neurosci* **40**, 8042-8054 (2020).
12. O. M. Lazo *et al.*, BDNF regulates Rab11-mediated recycling endosome dynamics to induce dendritic branching. *J Neurosci* **33**, 6112-6122 (2013).
13. G. Moya-Alvarado, A. Gonzalez, N. Stuardo, F. C. Bronfman, Brain-Derived Neurotrophic Factor (BDNF) Regulates Rab5-Positive Early Endosomes in Hippocampal Neurons to Induce Dendritic Branching. *Front Cell Neurosci* **12**, 493 (2018).
14. K. Deinhardt *et al.*, Rab5 and Rab7 control endocytic sorting along the axonal retrograde transport pathway. *Neuron* **52**, 293-305 (2006).
15. K. Zhang *et al.*, Defective axonal transport of Rab7 GTPase results in dysregulated trophic signaling. *J Neurosci* **33**, 7451-7462 (2013).
16. K. Barford *et al.*, Transcytosis of TrkA leads to diversification of dendritic signaling endosomes. *Sci Rep* **8**, 4715 (2018).
17. M. Ye, K. M. Lehigh, D. D. Ginty, Multivesicular bodies mediate long-range retrograde NGF-TrkA signaling. *Elife* **7**, (2018).

18. B. Zhou, Q. Cai, Y. Xie, Z. H. Sheng, Snapin recruits dynein to BDNF-TrkB signaling endosomes for retrograde axonal transport and is essential for dendrite growth of cortical neurons. *Cell Rep* **2**, 42-51 (2012).
19. M. A. Olenick, R. Dominguez, E. L. F. Holzbaur, Dynein activator Hook1 is required for trafficking of BDNF-signaling endosomes in neurons. *J Cell Biol* **218**, 220-233 (2019).
20. L. Goto-Silva *et al.*, Retrograde transport of Akt by a neuronal Rab5-APPL1 endosome. *Sci Rep* **9**, 2433 (2019).
21. E. J. Huang, L. F. Reichardt, Trk receptors: roles in neuronal signal transduction. *Annu Rev Biochem* **72**, 609-642 (2003).
22. D. R. Kaplan, F. D. Miller, Neurotrophin signal transduction in the nervous system. *Current opinion in neurobiology* **10**, 381-391 (2000).
23. G. M. Schratt, E. A. Nigh, W. G. Chen, L. Hu, M. E. Greenberg, BDNF regulates the translation of a select group of mRNAs by a mammalian target of rapamycin-phosphatidylinositol 3-kinase-dependent pathway during neuronal development. *J Neurosci* **24**, 7366-7377 (2004).
24. A. Gonzalez, G. Moya-Alvarado, C. Gonzalez-Billaut, F. C. Bronfman, Cellular and molecular mechanisms regulating neuronal growth by brain-derived neurotrophic factor. *Cytoskeleton (Hoboken)* **73**, 612-628 (2016).
25. N. Nandagopal, P. P. Roux, Regulation of global and specific mRNA translation by the mTOR signaling pathway. *Translation (Austin)* **3**, e983402 (2015).
26. M. S. Fernandopulle, J. Lippincott-Schwartz, M. E. Ward, RNA transport and local translation in neurodevelopmental and neurodegenerative disease. *Nat Neurosci* **24**, 622-632 (2021).
27. A. L. Kalinski *et al.*, mRNAs and Protein Synthetic Machinery Localize into Regenerating Spinal Cord Axons When They Are Provided a Substrate That Supports Growth. *The Journal of neuroscience : the official journal of the Society for Neuroscience* **35**, 10357-10370 (2015).
28. S. Koley, M. Rozenbaum, M. Fainzilber, M. Terenzio, Translating regeneration: Local protein synthesis in the neuronal injury response. *Neurosci Res* **139**, 26-36 (2019).
29. V. A. Bauer, M. Koppers, Multi-organelle-mediated mRNA localization in neurons and links to disease. *Curr Opin Genet Dev* **92**, 102332 (2025).
30. G. Moya-Alvarado *et al.*, PLC-γ-Ca2+ pathway regulates axonal TrkB endocytosis and is required for long-distance propagation of BDNF signaling. *Frontiers in Molecular Neuroscience* **17**, (2024).
31. J. P. Lezana *et al.*, Axonal PPARgamma promotes neuronal regeneration after injury. *Dev Neurobiol* **76**, 688-701 (2016).
32. C. A. Escudero *et al.*, c-Jun N-terminal kinase (JNK)-dependent internalization and Rab5-dependent endocytic sorting mediate long-distance retrograde neuronal death induced by axonal BDNF-p75 signaling. *Sci Rep* **9**, 6070 (2019).
33. D. L. Shelton *et al.*, Human trks: molecular cloning, tissue distribution, and expression of extracellular domain immunoadhesins. *J Neurosci* **15**, 477-491 (1995).
34. Q. Liu *et al.*, Discovery of 1-(4-(4-Propionylpiperazin-1-yl)-3-(trifluoromethyl)phenyl)-9-(quinolin-3-yl)benzo[h][1,6]naphthyridin-2(1H)-one as a Highly Potent, Selective Mammalian Target of Rapamycin (mTOR) Inhibitor for the Treatment of Cancer. *Journal of Medicinal Chemistry* **53**, 7146-7155 (2010).
35. S. tom Dieck *et al.*, Direct visualization of newly synthesized target proteins in situ. *Nat Methods* **12**, 411-414 (2015).

36. A. P. Grollman, Inhibitors of protein biosynthesis. II. Mode of action of anisomycin. *J Biol Chem* **242**, 3226-3233 (1967).
37. T. Wang *et al.*, Flux of signalling endosomes undergoing axonal retrograde transport is encoded by presynaptic activity and TrkB. *Nat Commun* **7**, 12976 (2016).
38. G. Moya-Alvarado, A. Aguirre-Soto, F. C. Bronfman, Multiple Labeling of Compartmentalized Cortical Neurons in Microfluidic Chambers. *Bio Protoc* **14**, e4911 (2024).
39. N. G. Gracias, N. J. Shirkey-Son, U. Hengst, Local translation of TC10 is required for membrane expansion during axon outgrowth. *Nat Commun* **5**, 3506 (2014).
40. K. Y. Wu *et al.*, Local translation of RhoA regulates growth cone collapse. *Nature* **436**, 1020-1024 (2005).
41. S. J. Lee *et al.*, Selective axonal translation of the mRNA isoform encoding prenylated Cdc42 supports axon growth. *J Cell Sci* **134**, (2021).
42. T. Altman *et al.*, Axonal TDP-43 condensates drive neuromuscular junction disruption through inhibition of local synthesis of nuclear encoded mitochondrial proteins. *Nat Commun* **12**, 6914 (2021).
43. X. Chen *et al.*, A chemical-genetic approach to studying neurotrophin signaling. *Neuron* **46**, 13-21 (2005).
44. D. Villarroel-Campos, G. Schiavo, O. M. Lazo, The many disguises of the signalling endosome. *FEBS Lett* **592**, 3615-3632 (2018).
45. E. Santini, T. N. Huynh, E. Klann, Mechanisms of translation control underlying long-lasting synaptic plasticity and the consolidation of long-term memory. *Prog Mol Biol Transl Sci* **122**, 131-167 (2014).
46. D. J. Mitchell *et al.*, Trk activation of the ERK1/2 kinase pathway stimulates intermediate chain phosphorylation and recruits cytoplasmic dynein to signaling endosomes for retrograde axonal transport. *J Neurosci* **32**, 15495-15510 (2012).
47. N. Panayotis, A. Karpova, M. R. Kreutz, M. Fainzilber, Macromolecular transport in synapse to nucleus communication. *Trends Neurosci* **38**, 108-116 (2015).
48. H. L. Zhang *et al.*, Neurotrophin-induced transport of a beta-actin mRNP complex increases beta-actin levels and stimulates growth cone motility. *Neuron* **31**, 261-275 (2001).
49. H. H. Wong *et al.*, RNA Docking and Local Translation Regulate Site-Specific Axon Remodeling In Vivo. *Neuron* **95**, 852-868.e858 (2017).
50. A. M. Taylor *et al.*, Axonal mRNA in uninjured and regenerating cortical mammalian axons. *J Neurosci* **29**, 4697-4707 (2009).
51. M. Koppers *et al.*, Axonal endoplasmic reticulum tubules control local translation via P180/RRBP1-mediated ribosome interactions. *Dev Cell* **59**, 2053-2068.e2059 (2024).
52. T. Shigeoka *et al.*, Dynamic Axonal Translation in Developing and Mature Visual Circuits. *Cell* **166**, 181-192 (2016).
53. R. Cagnetta, C. K. Frese, T. Shigeoka, J. Krijgsveld, C. E. Holt, Rapid Cue-Specific Remodeling of the Nascent Axonal Proteome. *Neuron* **99**, 29-46.e24 (2018).
54. A. S. Hafner, P. G. Donlin-Asp, B. Leitch, E. Herzog, E. M. Schuman, Local protein synthesis is a ubiquitous feature of neuronal pre- and postsynaptic compartments. *Science* **364**, (2019).
55. A. F. R. Batista, J. C. Martínez, U. Hengst, Intra-axonal Synthesis of SNAP25 Is Required for the Formation of Presynaptic Terminals. *Cell Rep* **20**, 3085-3098 (2017).
56. H. H. Wong, A. J. Watt, P. J. Sjöström, Synapse-specific burst coding sustained by local axonal translation. *Neuron* **112**, 264-276.e266 (2024).

57. A. Poulopoulos *et al.*, Subcellular transcriptomes and proteomes of developing axon projections in the cerebral cortex. *Nature* **565**, 356-360 (2019).
58. M. X. Li, J. W. Weng, E. S. Ho, S. F. Chow, C. K. Tsang, Brain delivering RNA-based therapeutic strategies by targeting mTOR pathway for axon regeneration after central nervous system injury. *Neural Regen Res* **17**, 2157-2165 (2022).
59. M. Terenzio *et al.*, Locally translated mTOR controls axonal local translation in nerve injury. *Science* **359**, 1416-1421 (2018).
60. Y. Lu, S. Belin, Z. He, Signaling regulations of neuronal regenerative ability. *Curr Opin Neurobiol* **27**, 135-142 (2014).
61. C. Bucci *et al.*, The small GTPase rab5 functions as a regulatory factor in the early endocytic pathway. *Cell* **70**, 715-728 (1992).
62. H. Horiuchi *et al.*, A novel Rab5 GDP/GTP exchange factor complexed to Rabaptin-5 links nucleotide exchange to effector recruitment and function. *Cell* **90**, 1149-1159 (1997).
63. B. Sonnichsen, S. De Renzis, E. Nielsen, J. Rietdorf, M. Zerial, Distinct membrane domains on endosomes in the recycling pathway visualized by multicolor imaging of Rab4, Rab5, and Rab11. *J Cell Biol* **149**, 901-914 (2000).
64. S. de Renzis, B. Sonnichsen, M. Zerial, Divalent Rab effectors regulate the sub-compartmental organization and sorting of early endosomes. *Nat Cell Biol* **4**, 124-133 (2002).
65. Y. Diekmann *et al.*, Thousands of rab GTPases for the cell biologist. *PLoS Comput Biol* **7**, e1002217 (2011).
66. Y. Homma *et al.*, Comprehensive knockout analysis of the Rab family GTPases in epithelial cells. *J Cell Biol* **218**, 2035-2050 (2019).
67. M. Elias, A. Brighouse, C. Gabernet-Castello, M. C. Field, J. B. Dacks, Sculpting the endomembrane system in deep time: high resolution phylogenetics of Rab GTPases. *J Cell Sci* **125**, 2500-2508 (2012).
68. A. Zeigerer *et al.*, Rab5 is necessary for the biogenesis of the endolysosomal system in vivo. *Nature* **485**, 465-470 (2012).
69. Y. Shi *et al.*, Haploinsufficiency leads to neurodegeneration in C9ORF72 ALS/FTD human induced motor neurons. *Nat Med* **24**, 313-325 (2018).
70. W. Xu, F. Fang, J. Ding, C. Wu, Dysregulation of Rab5-mediated endocytic pathways in Alzheimer's disease. *Traffic* **19**, 253-262 (2018).
71. R. S. Devon *et al.*, Als2-deficient mice exhibit disturbances in endosome trafficking associated with motor behavioral abnormalities. *Proc Natl Acad Sci U S A* **103**, 9595-9600 (2006).
72. S. Gluska, M. Chein, N. Rotem, A. Ionescu, E. Perlson, Tracking Quantum-Dot labeled neurotropic factors transport along primary neuronal axons in compartmental microfluidic chambers. *Methods Cell Biol* **131**, 365-387 (2016).

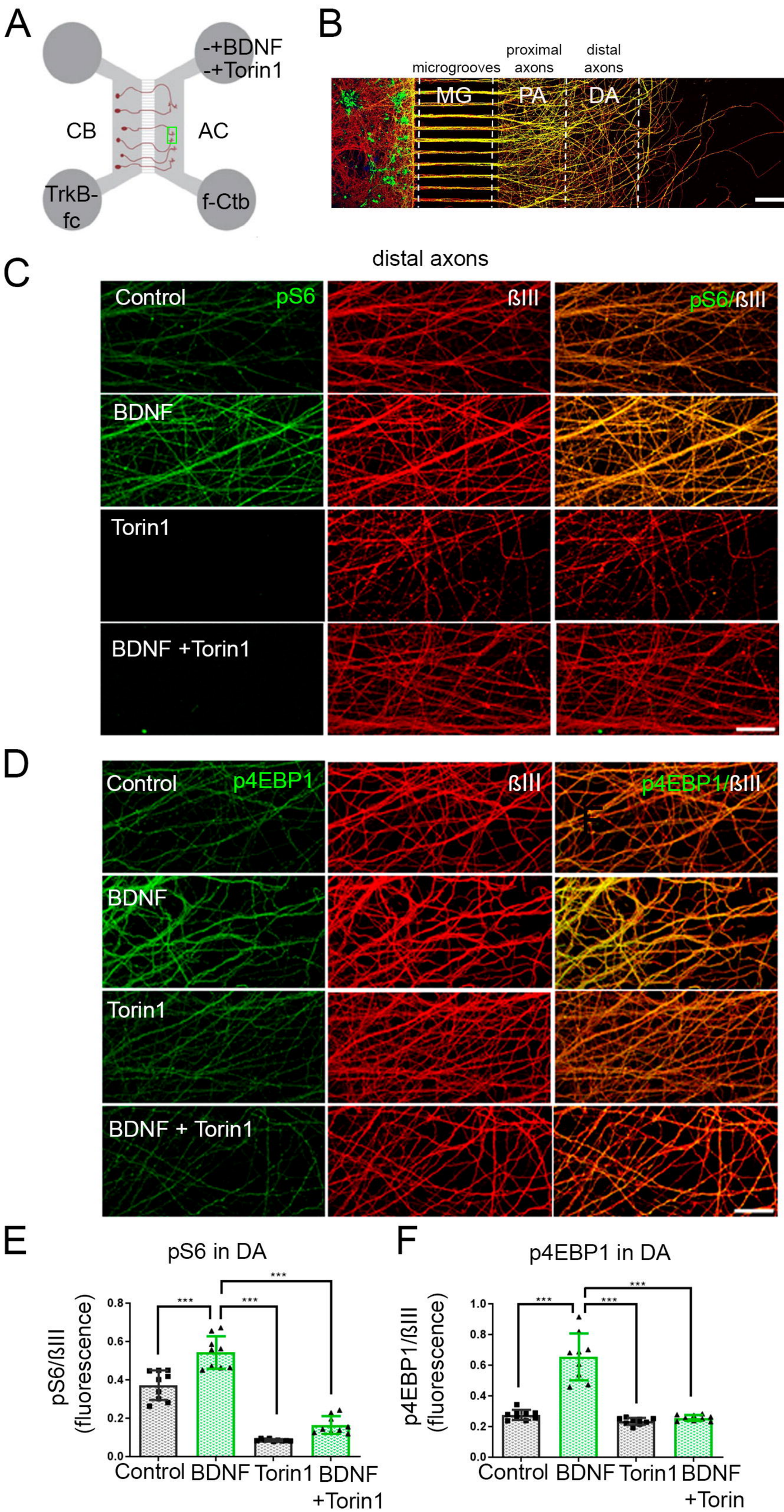
A
-+BDNF
-+Torin1
CB
AC
TrkB-fc
f-Ctb
B
microgrooves
proximal axons
distal axons
MG
PA
DA
C
distal axons
Control
pS6
ßIII
pS6/ßIII
BDNF
Torin1
BDNF +Torin1
D
Control
p4EBP1
ßIII
p4EBP1/ßIII
BDNF
Torin1
BDNF + Torin1
E
pS6 in DA
pS6/ßIII (fluorescence)
0.0
0.2
0.4
0.6
0.8
***
***
***
Control
BDNF
Torin1
BDNF +Torin1
F
p4EBP1 in DA
p4EBP1/ßIII (fluorescence)
0.0
0.2
0.4
0.6
0.8
1.0
***
***
***
Control
BDNF
Torin1
BDNF +Torin

A

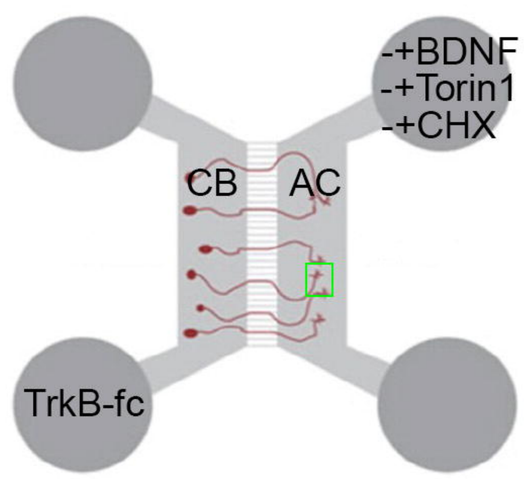
-+BDNF
-+Torin1
-+CHX
CB
AC
TrkB-fc

B

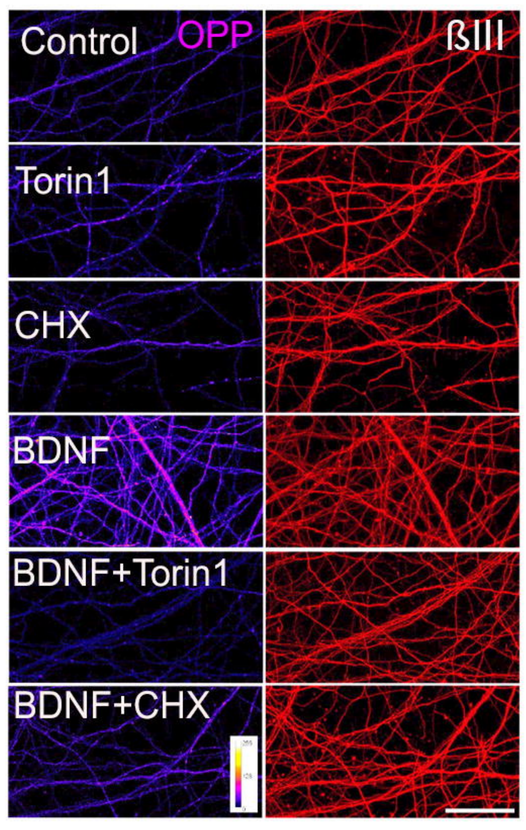
Control
OPP
ßIII
Torin1
CHX
BDNF
BDNF+Torin1
BDNF+CHX

C

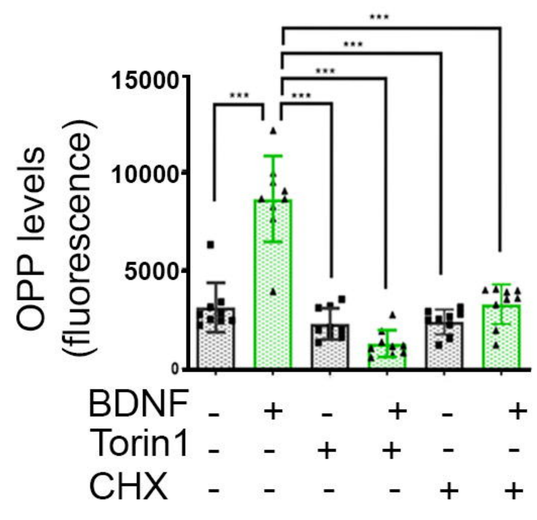
OPP levels
(fluorescence)
15000
10000
5000
0
***
BDNF - + - + - +
Torin1 - - + + - -
CHX - - - - + +

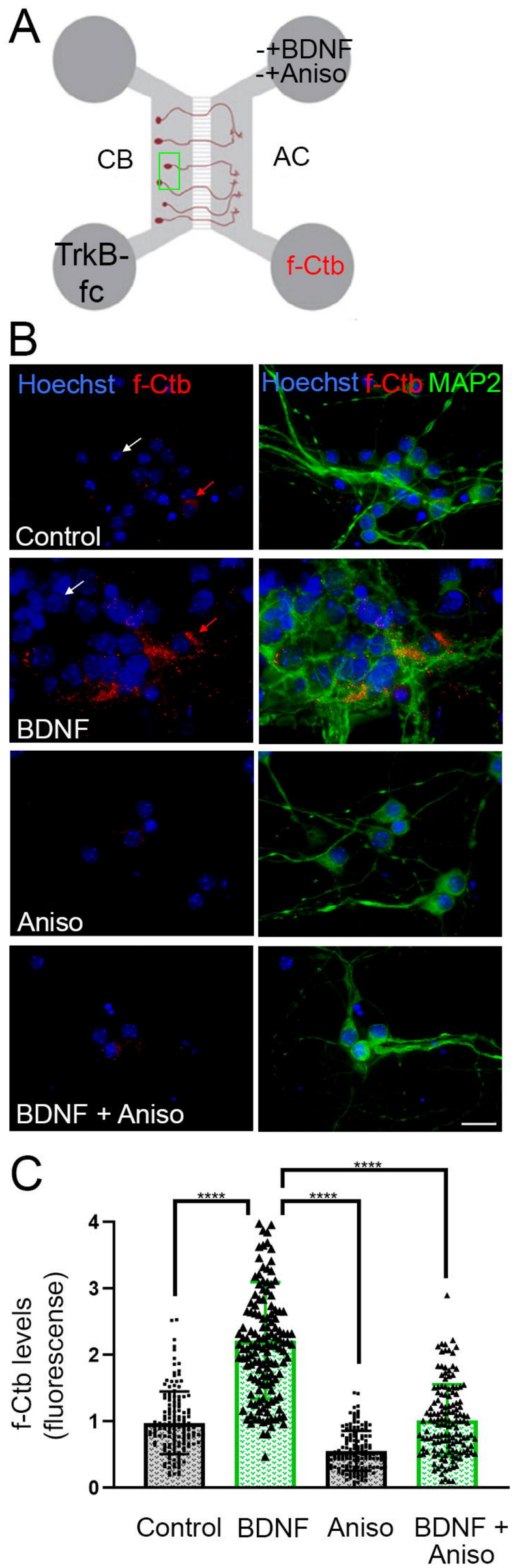
A
-+BDNF
-+Aniso
CB
AC
TrkB-fc
f-Ctb
B
Hoechst f-Ctb
Hoechst f-Ctb MAP2
Control
BDNF
Aniso
BDNF + Aniso
C
f-Ctb levels (fluorescense)
0
1
2
3
4
****
****
****
Control
BDNF
Aniso
BDNF + Aniso

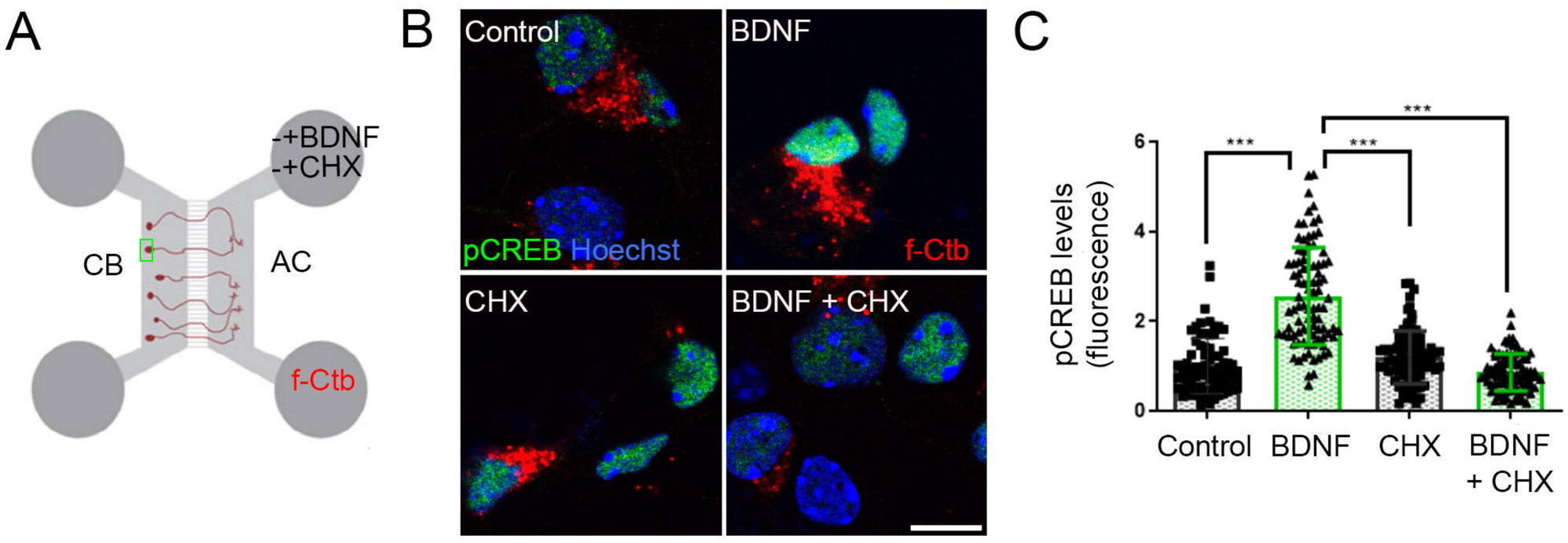
A
-+BDNF
-+CHX
CB
AC
f-Ctb
B
Control
BDNF
pCREB Hoechst
f-Ctb
CHX
BDNF + CHX
C
pCREB levels
(fluorescence)
6
4
2
0
***
***
***
Control
BDNF
CHX
BDNF
+ CHX

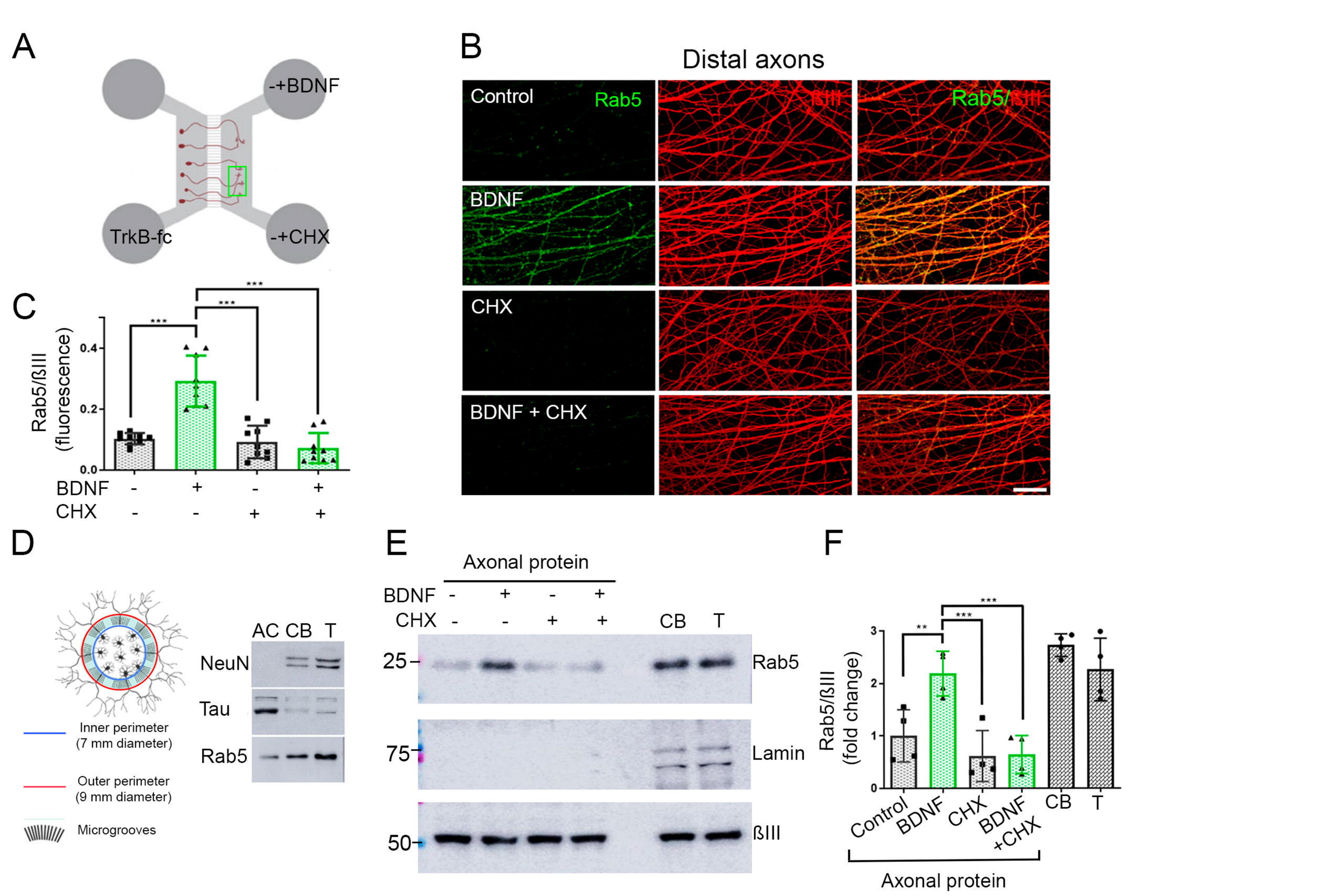
A
-+BDNF
TrkB-fc
-+CHX
B
Distal axons
Control
Rab5
ßIII
Rab5/ßIII
BDNF
CHX
BDNF + CHX
C
Rab5/ßIII (fluorescence)
0.0
0.2
0.4
***
***
***
BDNF - + - +
CHX - - + +
D
Inner perimeter (7 mm diameter)
Outer perimeter (9 mm diameter)
Microgrooves
AC CB T
NeuN
Tau
Rab5
E
Axonal protein
BDNF - + - +
CHX - - + +
CB T
25
75
50
Rab5
Lamin
ßIII
F
Rab5/ßIII (fold change)
0
1
2
3
**
***
***
Control
BDNF
CHX
BDNF +CHX
CB
T
Axonal protein

A

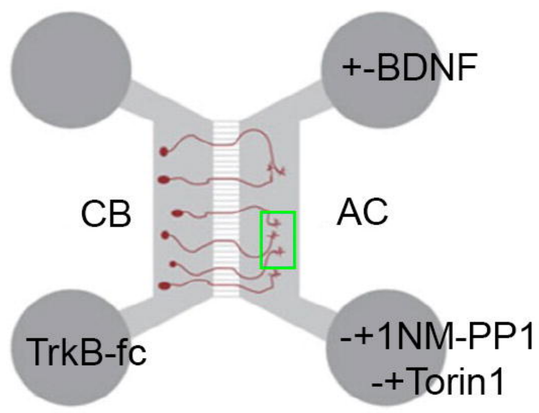
+-BDNF
CB
AC
TrkB-fc
-+1NM-PP1
-+Torin1

B

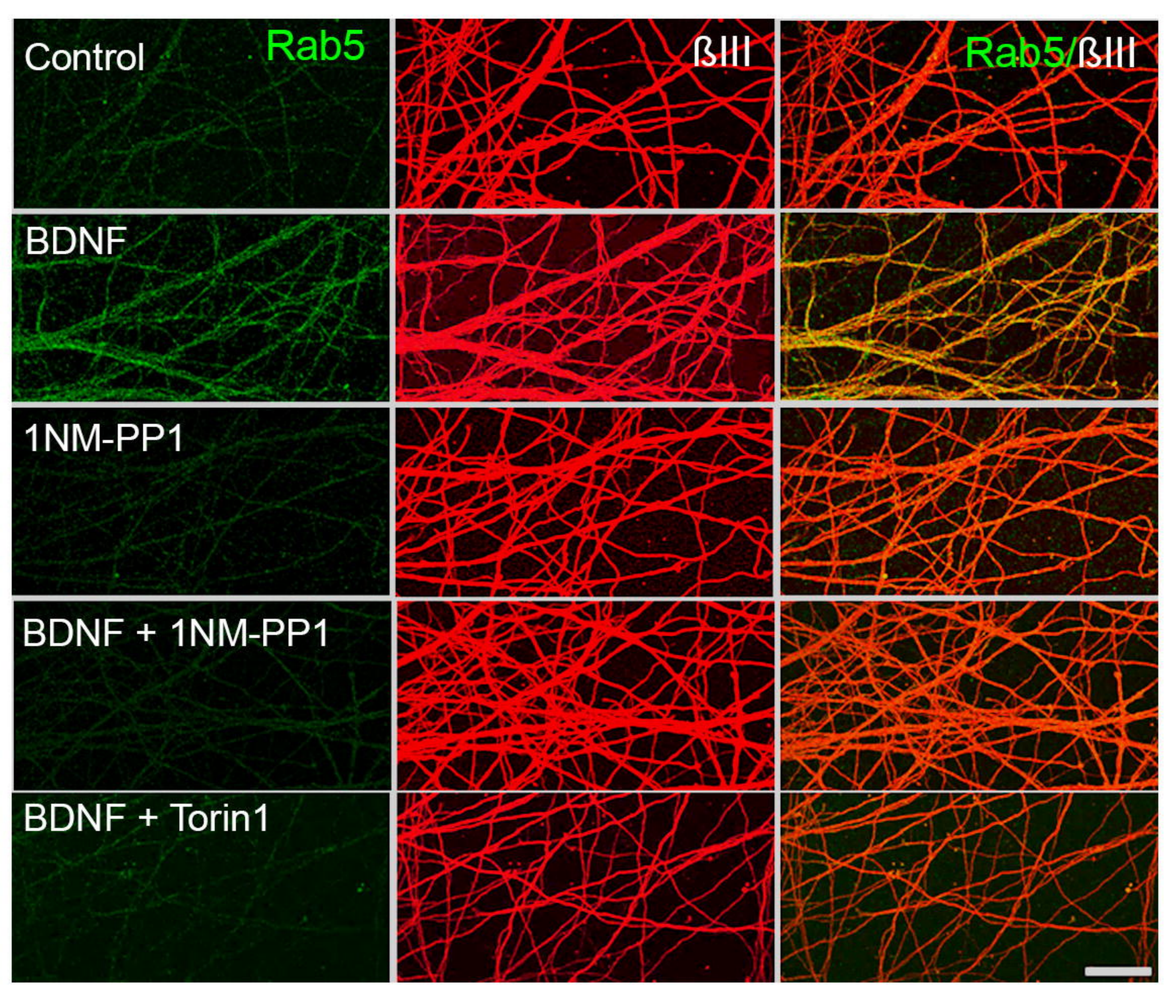
Distal axons
Control
Rab5
ßIII
Rab5/ßIII
BDNF
1NM-PP1
BDNF + 1NM-PP1
BDNF + Torin1

C

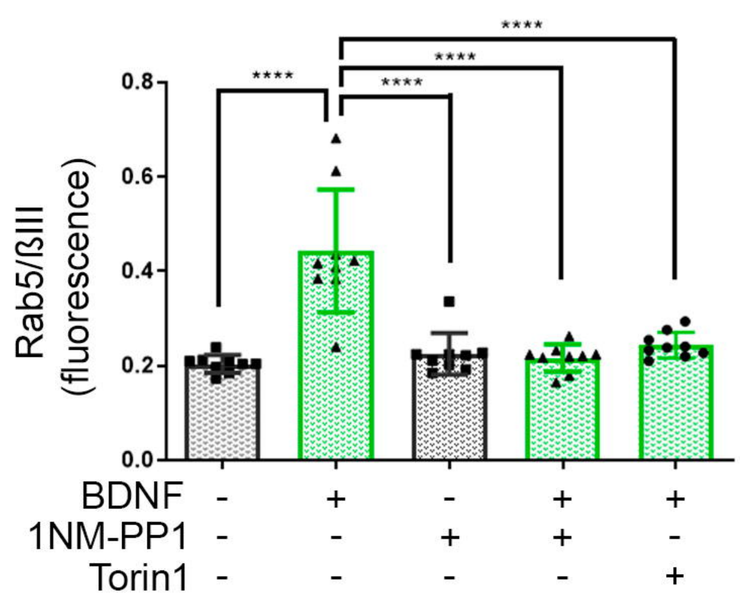
Rab5/ßIII
(fluorescence)
0.0
0.2
0.4
0.6
0.8
****
****
****
****
BDNF - + - + +
1NM-PP1 - - + + -
Torin1 - - - - +

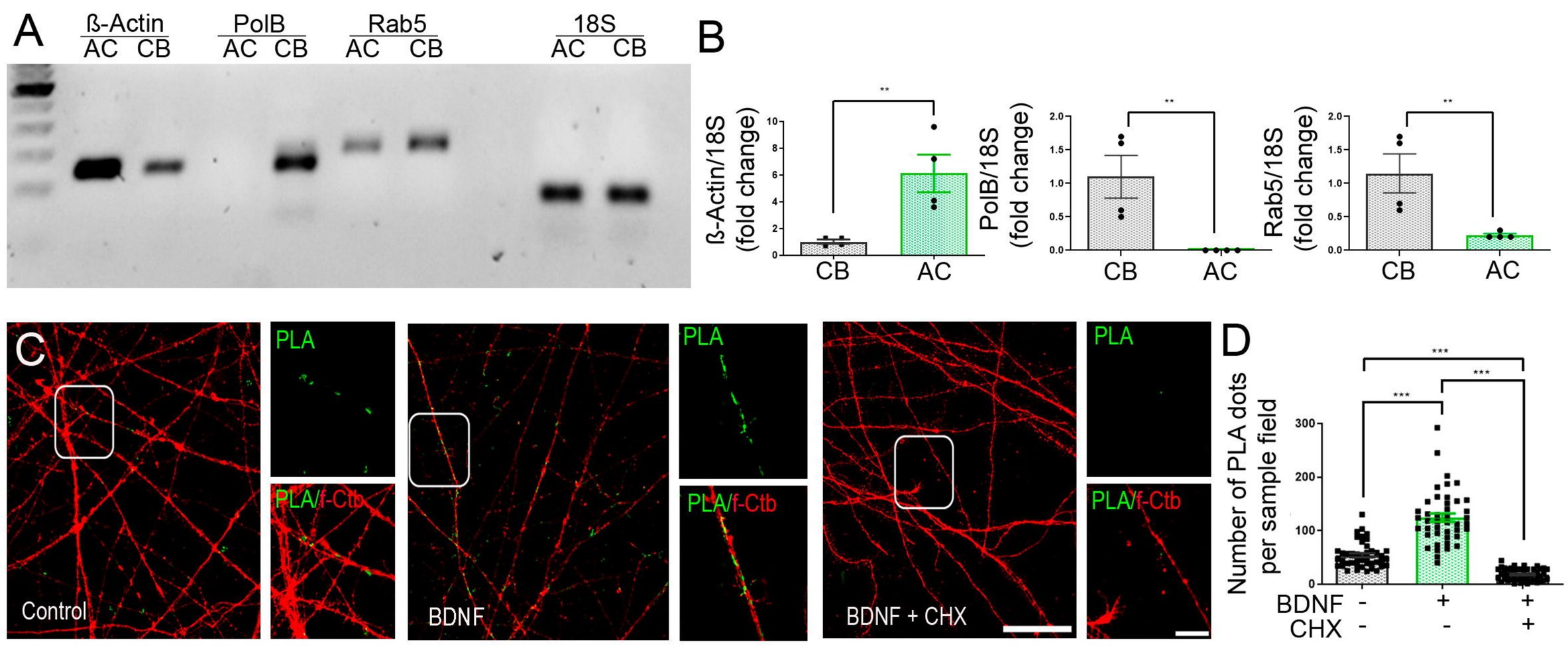
A
ß-Actin
AC CB
PolB
AC CB
Rab5
AC CB
18S
AC CB
B
ß-Actin/18S (fold change)
PolB/18S (fold change)
Rab5/18S (fold change)
CB
AC
C
PLA
PLA/f-Ctb
Control
BDNF
BDNF + CHX
D
Number of PLA dots per sample field
BDNF
CHX